

Development of a Wood Material Model For Roadside Safety Applications

Yvonne D. Murray
Aptek Inc
1257 Lake Plaza Drive
Colorado Springs, CO 80906
Voice/Fax: 719-576-8100/8252
yvonne@aptek.com

Abbreviations:

FHWA Federal Highway
FPL Forest Products Laboratory
MC Moisture Content
MOE Modulus of Elasticity
MWRSF Midwest Roadside Safety Facility

Key Words:

Damage, Model, Plasticity, Rate Effects, Transversely Isotropic, Wood

This document is disseminated under the sponsorship of the Department of Transportation in the interest of information exchange. The United States Government assumes no liability for its content or use thereof. This report does not constitute a standard, specification, or regulation.

The United States Government does not endorse products or manufacturers. Trade and manufacturers' names appear in this report only because they are considered essential to the object of the document.

ABSTRACT

A computationally efficient wood material model is being developed and validated for performing LS-DYNA simulations of vehicle collisions into wooden guardrail posts. Typically, the failure modes and stress-strain relationships of wood depend on the direction of the load relative to the grain and the type of load (tension, compression, or shear). The model includes transversely isotropic constitutive equations and yield surfaces to simulate different stiffnesses and strengths parallel and perpendicular to the grain. Hardening and softening formulations simulate stress-strain relationships that are linear to brittle failure in tension and shear, and nonlinear and ductile in compression. A rate effects formulation increases strength with strain rate. For easy use, default material properties for Southern yellow pine and Douglas fir are provided as a function of moisture content, temperature, and grade. Correlations with static bending and bogie impact tests are being used to validate the model.

INTRODUCTION

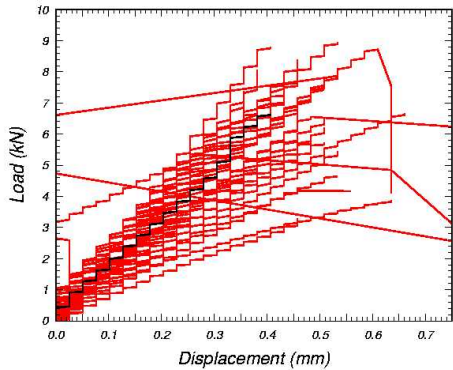
This work is part of a coordinated effort. The Federal Highway (FHWA) Technical Monitor is Dr. Martin Hargrave. Development and preliminary evaluation of the wood material model are being conducted by Ms. Murray of APTEK. The APTEK Program Manager is Dr. Brett Lewis. Material property data for Southern yellow pine and Douglas fir are provided by Drs. Mike Ritter and David Kretschmann of the Forests Products Laboratory (FPL) [Kretschmann & Green, 1996]. Static bending and dynamic bogie test data for wooden guardrail posts are provided by Drs. John Reid, Dean Sicking, and Ronald Faller of the Midwest Roadside Safety Facility (MWRSF) [Rhode & Reid, 1997]. The MWRSF personnel also plan to validate the wood material model by performing LS-DYNA simulations of the static and dynamic impact tests.

Variability of Wood

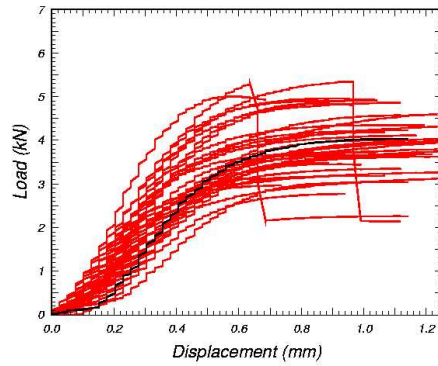
Wood is a highly variable material. This is usually due to natural variations in density, the presence of latewood and earlywood growth rings, and defects and growth characteristics such as knots, checks (split across rings), and shakes (split between rings). Wood of similar mechanical properties is grouped by stress grade.

In general, the stiffness and strength of wood varies with orientation between the longitudinal, tangential, and radial directions. The longitudinal direction is the fiber or grain direction. Stiffness and strength are greatest in the fiber direction. The tangential and radial directions are transverse to the fiber direction, and parallel and perpendicular to the growth rings. For modeling purposes, the distinction between the tangential and radial directions is not always significant. Therefore, this paper uses the term “perpendicular” to the grain when no distinction is made between the radial and tangential directions, and “parallel” to the grain to describe the longitudinal direction.

A suite of material properties tests was conducted by the FPL on clear wood specimens of Southern yellow pine [Kretschmann & Green, 1996] as a function of moisture content (MC) between 4% and 23%. The suite includes tension and compression parallel and perpendicular to the grain, shear parallel to the grain, and Mode I and Mode II stress intensity factors perpendicular to the grain. Although clear wood specimens are small and free of defects, measured stiffnesses and strengths still vary by about a factor of two, as shown in Figure 1 at 12% moisture content. The FPL also developed empirical equations for the average strengths, stiffnesses, and fracture intensities as a function of moisture content. This was done by fitting quadratic equations through the data, as shown in Figure 2.

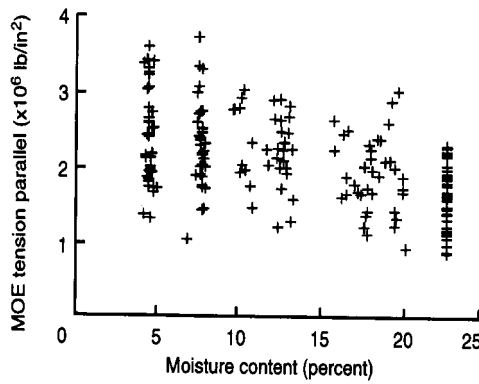


(a) Tension parallel.

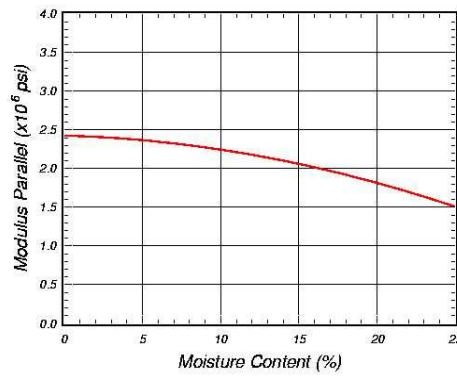


(b) Compression perpendicular.

Figure 1. These FPL measurements of clear wood Southern yellow pine specimens at 12% moisture content indicate about a factor of two variation in stiffness and strength.



(a) Data.



(b) Fit.

Figure 2. The empirical equations fit by the FPL to clear wood data are used as default material properties in the wood material model.

The failure modes and measured stress-strain relationships of wood depend on the direction of the load relative to the grain and the type of load (tension, compression, or shear). The stress-strain relationships of wood in parallel tension, perpendicular tension, and shear are typically linear to brittle failure, while the stress-strain relationship of wood in parallel compression and perpendicular compression are typically nonlinear and ductile, as shown in Figure 3 as a function of moisture content. These data are curves of average stiffness and strength, and are extracted from data sets like those previously shown in Figure 1. The data indicate up to a factor of three variation in strength with moisture content. Saturation refers to the fiber saturation point, which is approximately 23%.

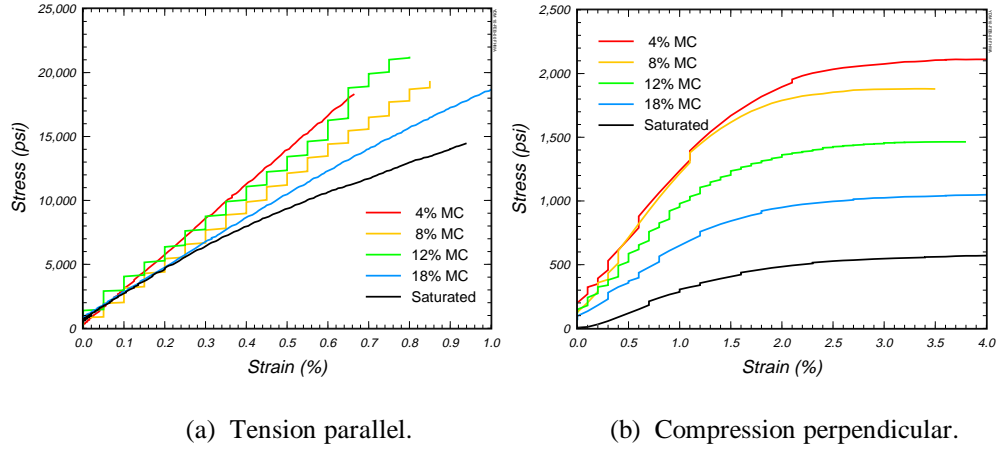


Figure 3. The FPL measured stress-strain relationships of Southern yellow pine depend on the load direction (parallel or perpendicular), load type (tensile, shear, or compressive), and the moisture content.

APPROACH

The wood material model consists of a number of formulations that are merged together to form a comprehensive model: elastic constitutive equations, yield surfaces, plasticity algorithms, hardening surfaces, damage-based softening, and rate effects.

Constitutive Equations

Elastic constitutive equations are implemented for a transversely isotropic material. Transverse isotropy is a subset of orthotropy. This means that the properties in two directions (tangential and radial) are modeled the same. The constitutive equations are formulated from five independent stiffness parameters.

Yield Surfaces

Two elliptical yield surfaces are implemented, one for yielding parallel to the grain, and the other for yielding perpendicular to the grain. Each yield surface is formulated from two of the five stress invariants of a transversely isotropic material. One stress invariant (determinant of the stress matrix) is neglected due to lack of data for defining its contribution. The yield surfaces are loosely based on the work of Hashin (1980). Each yield equation predicts yielding in tension, combined tension-shear, shear, combined compression-shear, and compression. The yield surfaces are formulated from six strength parameters.

Parallel Modes. Yielding occurs when $f_{\parallel} \geq 0$, where:

$$f_{\parallel} = \frac{\sigma_L^2}{X^2} + \frac{(\sigma_{LT}^2 + \sigma_{LR}^2)}{S_{\parallel}^2} - 1 \quad X = \begin{cases} X_T & \text{for } \sigma_L > 0 \\ X_C & \text{for } \sigma_L < 0 \end{cases} \quad (1)$$

Perpendicular Modes. Yielding occurs when $f_{\perp} \geq 0$, where:

$$f_{\perp} = \frac{(\sigma_R + \sigma_T)^2}{Y^2} + \frac{(\sigma_{RT}^2 - \sigma_R \sigma_T)}{S_{\perp}^2} - 1 \quad Y = \begin{cases} Y_T & \text{for } \sigma_R + \sigma_T > 0 \\ Y_C & \text{for } \sigma_R + \sigma_T < 0 \end{cases} \quad (2)$$

X_T	Tensile strength parallel to the grain
X_C	Compressive strength parallel to the grain
Y_T	Tensile strength perpendicular to the grain
Y_C	Compressive strength perpendicular to the grain
S_{\parallel}	Shear strength parallel to the grain
S_{\perp}	Shear strength perpendicular to the grain
σ_L	Longitudinal (parallel) stress
σ_R	Radial (perpendicular) stress
σ_T	Tangential (perpendicular) stress
σ_{LR}	Longitudinal-radial shear (parallel) stress
σ_{LT}	Longitudinal-tangential shear (parallel) stress
σ_{RT}	Radial-tangential shear (perpendicular)

Plasticity Algorithms

Plasticity algorithms are implemented which limit the stress state to lie on, and not outside, each yield surface. This is done by partitioning the strain tensor into elastic and plastic components through enforcement of the plastic consistency condition with associated flow (normal return to yield surface). No input parameters are required.

Hardening Surfaces

Pre-peak hardening formulations are implemented to simulate pre-peak nonlinearity in compression in the parallel and perpendicular modes. Hardening is modeled by defining an initial yield surface which hardens (translates) until it coincides with the ultimate yield surface. Two hardening parameters are required for each mode. The first parameter is the initial location of the yield surface which determines the onset of plasticity. The second parameter is the rate of translation of the yield surface which determines the nonlinearity.

Damage-Based Softening

Post-peak softening formulations are implemented to simulate strength and stiffness reductions in tension and shear. Softening is modeled using separate damage formulations for the parallel and perpendicular modes. The damage formulations are loosely based on the work of Simo and Ju (1987), *i.e.* $\sigma=(1-d)\underline{\sigma}$ where d is one of two strain-based damage parameters, $\underline{\sigma}$ is a stress component without damage (calculated by the plasticity algorithm prior to application of damage), and σ is a stress component with damage. Thus $1-d$ is a reduction factor associated with the amount of damage. Three input parameters are required for each damage formulation; the Mode I and II fracture energies, and a softening parameter which sets the shape of the softening curve. Mesh size dependency is regulated by explicitly including the element length in the damage formulation. Elements erode when the parallel damage parameter exceeds a value of $d=0.99$.

Rate Effects

High strain rate formulations are implemented for modeling strength enhancement at high strain rates. Two types of formulations are implemented, a Duvaut-Lions [1972] type viscoplastic formulation enhanced by Murray [1997], and a strain rate shifted yield surface formulation. Each formulation is based on two parameters for the parallel modes and two parameters for the perpendicular modes. The two parameters allow the user to fit dynamic data at two strain rates. Correlations with dynamic bogie test data will be used to set the default model parameters and determine the best formulation.

The behavior of the model is demonstrated in Figure 4 for the parallel modes. The behavior of the model for the perpendicular modes is qualitatively similar to that shown in Figure 4.

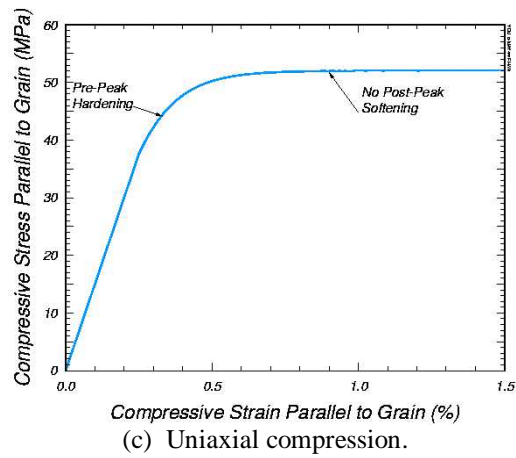
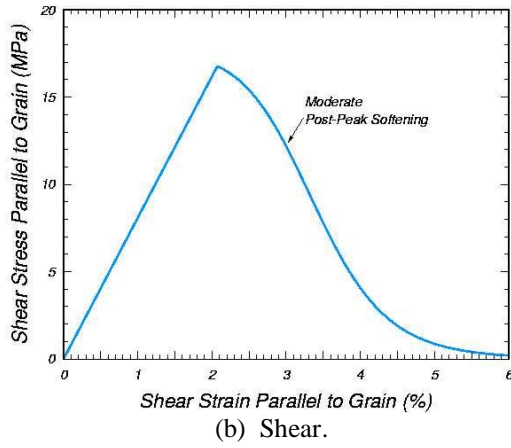
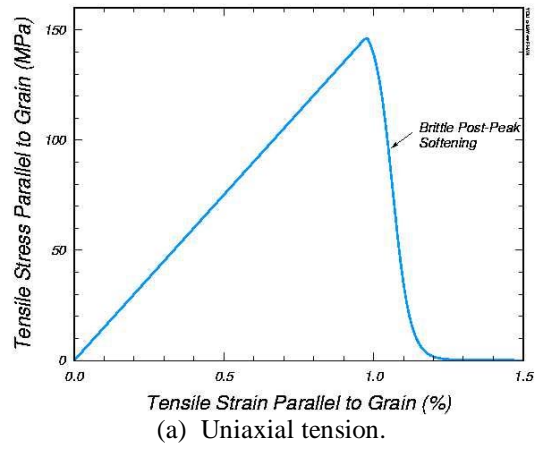


Figure 4. Calculated stress-strain response of Southern yellow pine demonstrating hardening and softening parallel to the grain.

Two methods are available for wood model input. One method is to input all 25 material property parameters. A second method is to request default material properties. This method is convenient because it allows the user to bypass the manual input of material parameters. Default material properties are provided for Southern Yellow pine and Douglas fir as a function of moisture content, temperature, and grade. Alternatively, in place of grade, the user may specify a strength reduction factor. The user can also choose units, activate the rate effects model, and specify the maximum number iterations performed by the plasticity algorithm.

DISCUSSION OF RESULTS

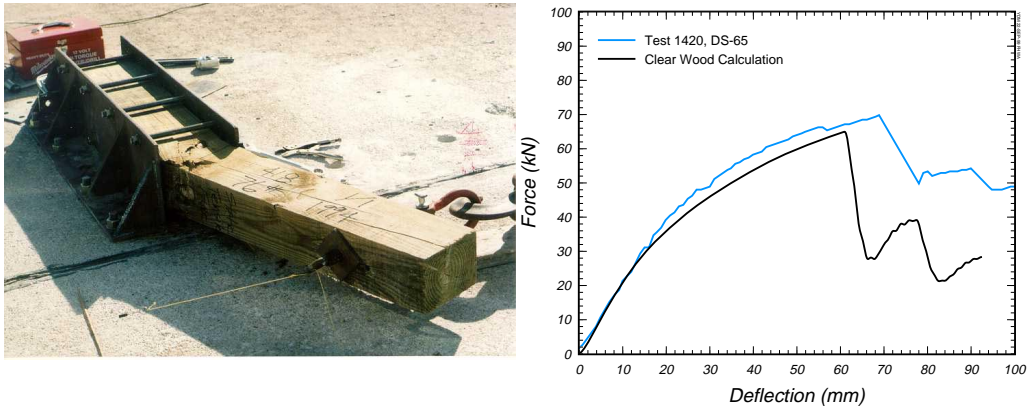
Static Bending Test Correlations

The MWRSF conducted 25 bending tests on Southern yellow pine posts of three grades (DS-65, 1D, 1) [Rhode & Reid, 1997]. The posts were removed from the field from guardrail installations. They were cantilevered in a rigid frame, and loaded at constant rate (Figure 5a). Load and deformation were continuously recorded. Post damage is dominated by tensile failure, particularly near the support. Peak force, deflection, and energy are listed in Table 1. Substantial scatter is observed in the data. For the DS-65 posts, all peak force, deflection, and energy measurements are within 20%, 37%, and 57% of the average measurements, respectively. For the Grade 1 posts, all peak force, deflection, and energy measurements are within 40%, 61%, and 66% of the average measurements, respectively.

Table 1. Average of MWRSF static post test data by grade.

Grade	Number of Posts	Peak Force		
		Force (kN)	Deflection (mm)	Energy (kN/m)
DS-65	10	67	68	3.04
1D	7	55	48	1.97
1	8	42	53	1.44

Comparison of one calculation with test data is shown in Figure 5b. The calculation is performed with default clear wood properties for room temperature, saturated pine. The data curve is from the DS-65 pine tests, and was selected because its peak force and deflection are close to the average measured values. Simplified boundary conditions are used (the rigid frame and neoprene padding are not modeled). The pre-peak calculation compares favorably with the data, although the post-peak calculation is more brittle than the data. Calculated damage is significant near the support, in agreement with the data. Two efforts are planned to improve the post-peak correlation. First, we will plot up all the data to identify an average post-peak response. Second, we will perform parametric calculations to provide a better post-peak correlation. An increase in the Mode I parallel to the grain fracture energy is expected to improve the correlation. The parallel fracture energy used in the calculation is an estimate (no measured values were available for use as default properties).



(a) Test apparatus. (b) Test data and calculation.

Figure 5. The model correlates well with the damage location and pre-peak test data, although an increase in the default parallel fracture energy is planned to improve the post-peak correlation.

Bogie Impact Test Correlations

The MWRSF conducted 80 bogie tests on Southern yellow pine posts of five grades (DS-65, 1D, 1, 2D, 2), and 7 tests on Douglas fir posts of one grade (1) [Rhode & Reid, 1997]. Significant knots and defects were cataloged. The posts were placed in a steel tube embedded in reinforced concrete (Figure 6a). The post/steel interface was padded with neoprene on the front and back. The posts were impacted at approximately 9.4 m/s by a 944 kg bogie. Impact force and deformation were derived from an accelerometer located on the bogie. Damaged posts were photographed (Figure 6b). Test results in Table 2 provide information on post performance versus grade. Comparisons of the dynamic bogie impact forces with the static bending forces also suggest a rate effect.



(a) Pre-test. (b) Post-test.

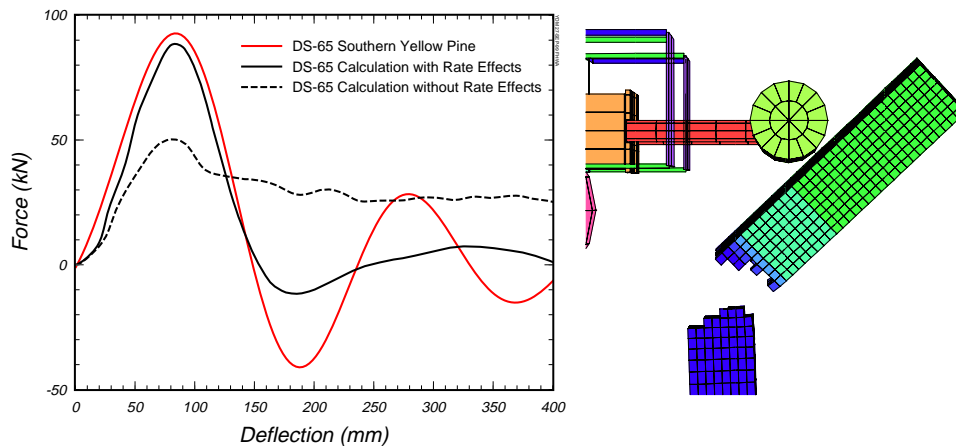
Figure 6. Pre-test wood post set-up and post-test DS-65 wood post damage for MWRSF bogie impact tests.

Table 2. Summary of MWRSF bogie impact tests on posts by grade.

No. of Posts	Grade	Peak Force				Rupture		
		Force (KN)	Time (ms)	Defl (mm)	Energy (KNmm)	Time (ms)	Defl (mm)	Energy (KNmm)
16	65	95	9.0	86.3	4428	18.8	170.2	8744
16	1D	49	8.2	78.7	2248	15.4	144.8	4180
9	1 – Worst	38	9.3	86.3	1853	18.0	162.6	3582
7	1 – Random	47	8.3	81.2	2135	15.5	149.9	4101
16	2D	52	8.6	83.8	2407	17.5	165.1	4723
16	2	44	9.1	88.9	2135	16.7	160.0	4011
7	Doug-Fir	46	8.4	81.2	2135	15.9	149.9	4044
5	Frozen-DS65	62	7.9	76.2	2666	14.5	139.7	5084
7	Frozen-1	43	7.9	76.2	1864	14.9	142.2	3530

Comparisons of two calculations with test data are shown in Figure 7, along with the calculated deformation at 40 msec. The calculations are performed with default clear wood properties for room temperature, saturated pine. Calculations are performed with and without modeling rate effects. Simplified boundary conditions were used (the steel tube and neoprene padding were not modeled). The data curve is from the DS-65 pine tests, and was selected because its peak force is close to the average measured value. The calculation without rate effects is in poor agreement with the measured data: the calculated force is approximately half the measured force. The calculation with rate effects is in reasonable agreement with the measured data, at least for the first 150 msec. The calculated response damps out quicker (is less elastic) than the measured response.

Two efforts are planned to improve the late time correlation. First, we will plot up all the data to identify a representative late time response. Second, we will perform parametric calculations to provide a better late time correlation. An increase in the Mode I parallel to the grain fracture energy, as planned for the static tests, is also expected to improve the dynamic correlation (make it damp out more slowly). The correlations indicate that modeling rate effects is necessary for wood post impact simulations.



(a) Test data and calculations.

(b) Calculated fracture.

Figure 7. The wood model calculation with rate effects correlates well with the first 150 msec of the measured force-deflection history, and with the measured fracture location.

SUMMARY AND CONCLUSIONS

A computationally efficient wood material model is being developed by APTEK for use in roadside safety applications. Tentative, quick look calculations have been performed by APTEK with the wood material model using default material properties and simplified boundary conditions. The model does a good job of simulating the behavior of saturated Southern yellow pine posts observed in static bending and dynamic bogie impact tests. A more thorough set of calculations will be performed by the MWRSF during the summer of 2000, including analyses of Douglas fir and frozen pine posts. Adjustments will be made to the default material properties and model formulations, as needed, to obtain good correlations with the test data. Once we are satisfied with the correlations, the wood material model will be forwarded to the Livermore Software Technology Corporation for inclusion in LS-DYNA. Documentation will include a User Manual, Theoretical Manual, and an Examples Manual.

REFERENCES

1. Duvaut, G. and J.L. Lions, "Les Inequations en Mechanique et en Physique," Dunod, Paris, 1972.
2. Green, D.W. and Kretschmann, "Moisture Content and the Properties of Clear Southern Pine, Research Paper FPL-RP-531," United States Department of Agriculture, Forest Products Laboratory.
3. Hashin, Z., "Failure Criteria for Unidirectional Fiber Composites," Transactions of the ASME, Journal of Applied Mechanics, June 1980, Vol. 47, pp. 329-334.
4. Kretschmann, D. E., and David W. Green, "Modeling Moisture Content-Mechanical Property Relationships for Clear Southern Pine," Wood and Fiber Science, 28(3), 1996, pp. 320-337.
5. Murray, Y. D., "Modeling Rate Effects in Rock and Concrete," Proceedings of the 8th International Symposium on Interaction of the Effects of Munitions with Structures, Defense Special Weapons Agency, McLean, VA, USA, April 1997.
6. Rhode, John and John Reid, "Evaluation of the Performance Criteria for Wood Posts in Strong-Post W-Beam Guardrail," Transportation Research Board Paper 971206, Jan. 1997.
7. Simo, J.C. and J.W. Ju, "Stress and Strain Based Continuum Damage Models," Parts I & II, Int. J. of Solids and Structures, Vol. 23, No. 7, 1987.